

A CSO Submillimeter Active Optics System

Melanie Leong ^a, Ruisheng Peng ^a, Martin Houde ^{a*}, Hiroshige Yoshida ^a, Richard Chamberlin ^a,
Thomas G. Phillips ^b

^a Caltech Submillimeter Observatory, 111 Nowelo Street, Hilo, HI 96720

^b California Institute of Technology, MC 320-47, 1200 E. California Blvd., Pasadena, CA 91125

ABSTRACT

Active surface correction of the Caltech Submillimeter Observatory (CSO) primary mirror has been accomplished. The Dish Surface Optimization System (DSOS) has been designed and built to operate at the CSO, on Mauna Kea, Hawaii. The DSOS is the only active optics system of its kind in the world. There are 99 steel rod standoffs that interface the dish panels to its backing structure. Each standoff is now fitted with a heating/cooling assembly. Applying a controlled potential to each of the 99 assemblies adjusts the surface of the dish. Heating elongates and cooling shortens the standoffs, providing the push or pull on the primary's panel surface. The needed correction for each standoff, for a given elevation, is determined from prior holography measurements of the dish surface. Without the DSOS the optimum surface accuracy was 25- μm RMS, yielding a beam efficiency of 33% at the 350- μm -wavelength range. With the DSOS on, this has been improved to 10- μm RMS. The best beam efficiency obtained is 56%, with an average beam efficiency of 53%. The DSOS has been in operation on the CSO since February 2003. Observers using the SHARCII (a 384 pixel submillimeter high angular resolution camera) and the 850 GHz heterodyne receiver, have been able to detect new weak and/or distant objects including detection of an earth-massed planet in Fomalhaut with the help of this unique active optics system.

Keywords: Active optics, submillimeter, radio telescopes, surface adjustment

1. INTRODUCTION

The Caltech Submillimeter Observatory (CSO) is equipped with a Leighton primary mirror [1] consisting of 84 hexagonal parabolic segments, together measuring 10.4 meters in diameter. By implementing a system that corrects gravitational deformations of the primary as it moves in elevation, close to twice the beam efficiency has been achieved. With an improved efficiency, the integration time will be reduced by a factor of four, or detection of more new deep-field objects could be achieved. A unique design, which can heat or cool individual steel rod standoffs of the primary, has been developed and is in use. It is named the Dish Surface Optimization System or DSOS.

2. SYSTEM DESIGN

On other telescope primary segments, mechanical worm drives are in use as active optics systems. Heating and cooling is an innovation to step away from mechanical gears. This helps preserve the primary's original alignment and tuning. If an observer prefers the dish without correction, the DSOS can be turned off, allowing the structure to return to its quiescent state.

The DSOS incorporates the use of thermal electric coolers or TECs. When a voltage is applied, the device will heat or cool the panel standoff rod, depending on the voltage's polarity. As a TEC heats or cools an assembly, an embedded thermistor is read. The thermistor level and desired setting are subtracted and their difference is used as the control level to the TEC. The voltage will stabilize to a value that will keep the error signal to zero. See Figure 1 for a block diagram of a single channel. Because the TEC is mounted on a precision structure at high altitude, heatsinks could not be used. To save on weight and to obtain a higher cooling capacity, a liquid heat exchanger with refrigerated bath, were incorporated into the TEC assembly.

* Presently at the University of Western Ontario, London, Ontario Canada N6A 3K7

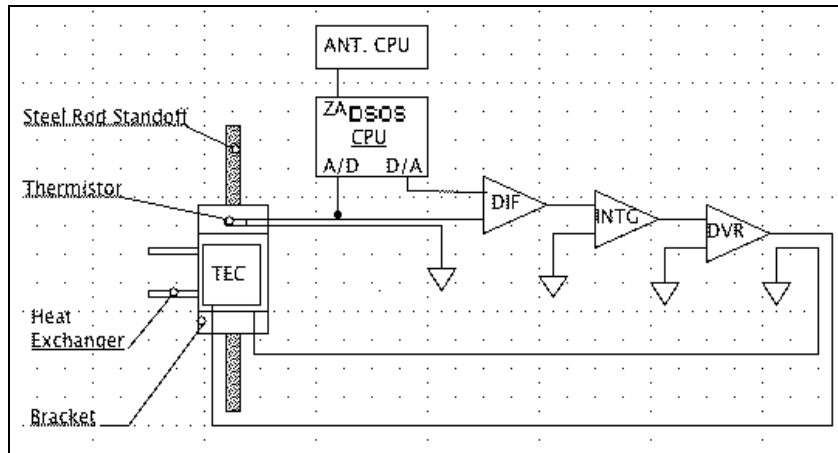


Figure 1. DSOS Simplified Block Diagram of a Single Channel. The thermistor level and desired setting are subtracted and their difference is used as the control level to the TEC.

3. SYSTEM DESCRIPTION

There are 99 steel rod standoffs that interface the dish to its backing structure. These standoffs are where the TEC assemblies are mounted. The assembly consists of a mounting bracket, embedded thermistor, TEC, and heat exchanger. The mounting bracket clamps around the steel rod standoff while giving the TEC a flat surface to mount to. See Figure 2. The bracket also has a glass bead thermistor embedded in it to supply feedback to the controller unit. A heat exchanger is mounted on the TEC to remove heat produced when cooling.



Figure 2a. TEC Assembly Installed on Primary Standoff

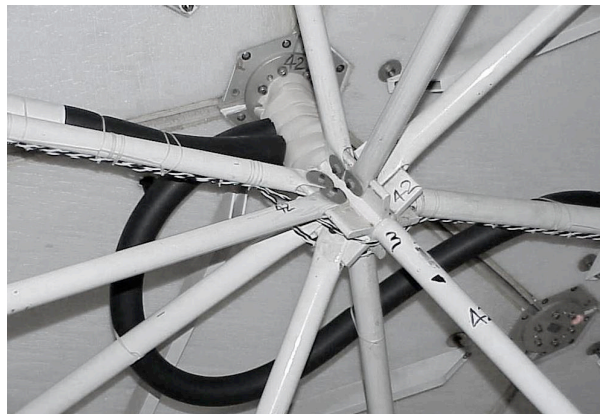


Figure 2b. Insulated TEC Assembly

In Figure 2a, the TEC Assembly is shown mounted on the back of the primary. The mounting bracket, liquid heat exchanger and wiring are visible. Figure 2b displays the TEC Assembly, fully insulated, including its coolant lines.

From the 99 TEC assemblies, routed along the dish backing structure, there are long wire harnesses for thermistor feedback and TEC power, plus lines of insulated tubing for plumbing the heat exchangers to their refrigerated baths. A 50/50 mixture of glycol and distilled water is used.

The rest of the system is located on the CSO's third floor mezzanine. This consists of a Controller rack, two Driver racks, two refrigerated baths for the Driver racks, four refrigerated baths for each quadrant of the dish, and their respective pump and manifold.

The 99 Channel Controller Unit houses (10) ten-channel controller PCBs. The controller's computer runs on a Linux OS with programs written in C and Fortran. The channels are selected via a zero card, containing a Xilinx chip that queries individual A/Ds and commands their respective D/As. The Controller Unit receives the thermistor levels from the TEC assemblies and outputs the difference between the thermistor reading and desired command setting. This control voltage is input to a power amplifier to drive the TECs. As the difference between the thermistor's voltage and the desired voltage setting gets driven to zero, so does the power driving each channel's TEC.

There are four 25 Channel Driver Units. Each unit is dual air and liquid cooled. This is due to 25 power amplifiers mounted on a large heatsink plate that operates at 13,800 feet altitude elevation. A single Driver Unit powers one quadrant of the dish. The dish is sectioned into four quadrants, for ease of integration and test, hardware groupings, and wiring purposes.



Figure 3. DSOS System Racks. 99 Channel Controller Rack, Center; Drivers & Power Supplies, Side Racks.

4. CALIBRATION, TABLES, AND VERIFICATION

The full DSOS build was completed in May 2002, 14 months after its start. This is a very fast completion time. Calibration of the 99 channels started in January 2003 and was completed in June 2003. As with the hardware build, where much time was spent climbing on the backing structure and installing all the assemblies, wiring, and coolant lines, the calibration was done “the old fashioned way,” with dial indicators, C-clamps to hold things together, multimeter, and binoculars when needed. The channels were calibrated one at a time and the data put into a spreadsheet

To begin the TEC assembly calibration, the starting temperature, length, and channel voltages are initialized and logged. The ambient temperature is recorded after the antenna is thermally equilibrated at the start of the evening, and is used as the reference for calibration. Starting values of length, voltage, temperature, then set values of length, voltage, and temperature, are recorded and used to calculate the factors (a, b, c) needed to construct a Resistance vs. Temperature curve for each TEC assembly. This is explained in the following text and equations.

By obtaining a thermistor's voltage, its resistance and thus its temperature can be determined. A thermistor's resistance, R_{th} , can be determined by:

$$R_{th} = V_{th} / 2.5 \mu A \quad (1)$$

V_{th} is obtained from the Controller Unit computer's A/D input. The thermistor loop is provided with a constant current source of $2.5 \mu A$. From the manufacturer's thermistor R vs. T curve, temperature can be determined. The change in length with temperature of each steel rod standoff is approximately:

$$\Delta L \approx \rho L \Delta T \quad (2)$$

From empirical measurements, it was found that $\rho L \approx 2.5 \mu m/^{\circ}C$. From the relation of equation (2), the length change for a given change in temperature is:

$$\Delta L = \Delta T \cdot 2.5 \quad (3)$$

$$(L_0 - L_{TP}) = (T_{th} - T_0) \cdot 2.5 \quad (4)$$

$$\Delta T = T_{th} - T_0 \quad (5)$$

ΔL is a length change of a standoff in microns. T_0 is the starting temperature (at ambient) where the length change = 0. ΔT is the change in standoff temperature from T_0 . T_{th} can be interpreted as the TEC assembly temperature, for a steel standoff length of L_{TP} . T_{th} is measured in terms of the resistance of the thermistor. The following is the Steinhart-Hart equation describing the resistance change of a thermistor as related to its temperature:

$$T_{th} = 1/a + b \cdot \ln(R) + c \cdot \ln(R^3) - 273 \quad (6)$$

Measured T_0 , V (at four voltage settings), and the respective standoff length changes are used to determine the values of a, b, and c in equation (6). R is determined by equation (7) where $I = 2.5 \mu A$ of a constant current source.

$$R = V / I \quad (7)$$

The curve derived from equation (6) is the calibrated fit to the TEC channel assembly. An example of TEC assembly calibration curves is shown below in Figure 4. Included for comparison, the leftmost curve (labeled 0) is made from the manufacturer's nominal values.

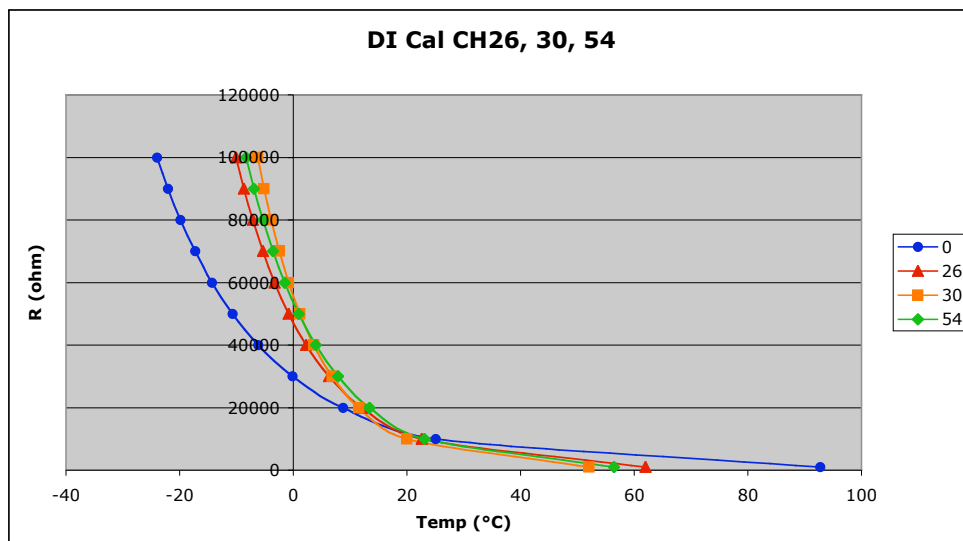


Figure 4. A Sample of Thermistor Calibration Curves. Three channels are displayed w/ the data sheet curve as “0.”

The a, b, and c values are stored and recalled during a dish correction call. The recalled values are used to calculate the thermistor target voltage for the desired ΔL . The ΔL in relation to zenith angle (ZA) are the cosine fits of measurements from past holography maps.

A quick summary flow is the following: present ZA > cosine fit lookup, $\Delta L > T(R, a, b, c) > V$ (new thermistor target voltage). The starting values of T_0 and V_0 are stored and used as the reference values for each new setting determination.

It is understood that there is a sinusoidal dependence caused by the changing gravity vector on the primary [2]. The zenith angle lookup tables are fashioned after this feature. The offset data points are a compilation of high confidence holography maps [2][3]. Each TEC assembly's calibration curve is adjusted in accordance to the zenith angle cosine curve. This is shown in equation (8) where the length change, in microns, is denoted by ΔL , α is the amplitude offset, za is the zenith angle, and β is the phase angle offset. Figure 5 shows this cosine fit to the holography data points.

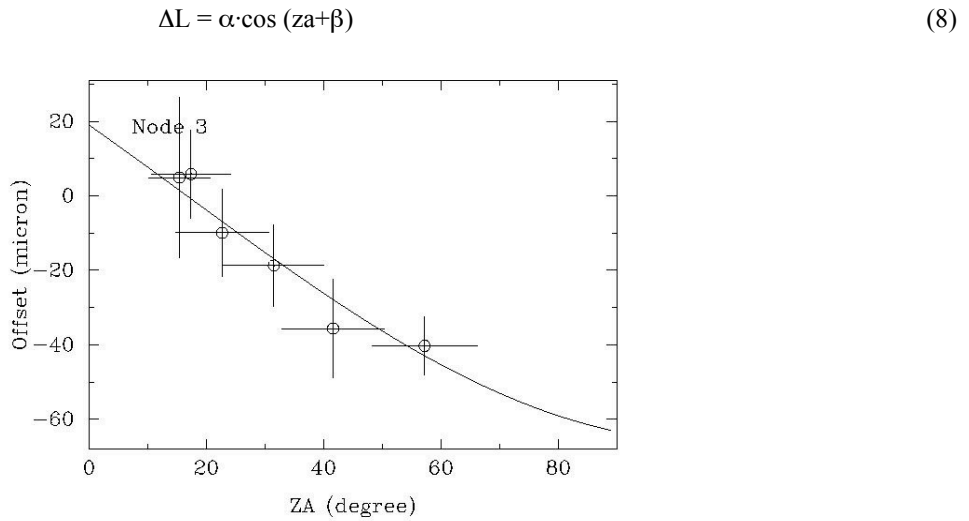


Figure 5. An Example of a Cosine Curve Fit to Holography Data Points.

In February 2003, signal power and full width half max (FWHM) improvements were measured from Ganymede, one of Jupiter's moons. This was done with 28 calibrated DSOS channels activated and the SHARCII [4]. The data was taken in the zenith angle range of 30 to 4 degrees, then 4 to 28 degrees. Signal power improved by as much as 50% and the best FWHM improvement was 3.4-arcsec from an originally 14-arcsec measurement. The best improvement occurred while the dish was in a small zenith angle range of 5 to 15 degrees. This is the range where the dish incurs more deformations from gravitational sag. The dish's mechanical tuning is in the 40 degree zenith angle range, so less improvement from the DSOS is expected there. Hysteresis of the primary occurs consistently, as the improvement on the descent is better than during ascent. See Figure 6. This performance was impressive due to the small number of activated channels to achieve such improvements. This verification gave confidence that the DSOS was working and well on its way.

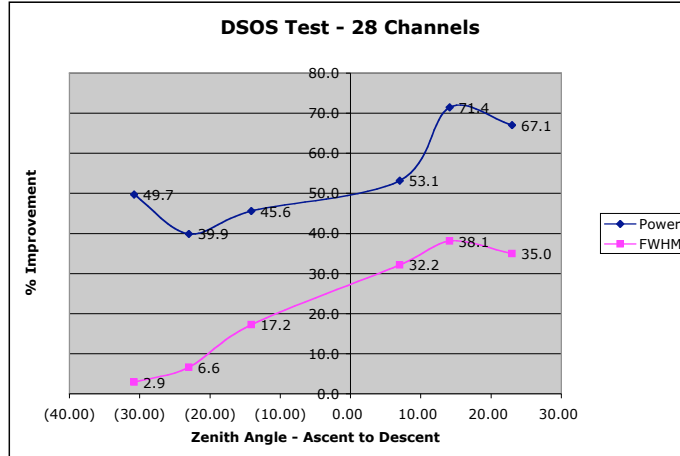


Figure 6. DSOS Performance Results with 28 Activated Channels. At small zenith angles the DSOS was able to improve the signal power by as much as 50%. Best FWHM improvement was 3.4-arcsec, with the telescope beam improved from 14-arcsec to 10.6-arcsec.

5. DSOS PERFORMANCE

The DSOS had 92 out of 99 operating channels in May 2004. Figure 7 displays improvements in the SHARCII maps. These are images of Ganymede, one of Jupiter's moons. The FWHM improved 18% from 10.4-arcsec to 8.8-arcsec. Peak signal power increased 50% from 64.6 Jy/Beam to 129 Jy/Beam. The zenith angle range is from 11 to 15 degrees.

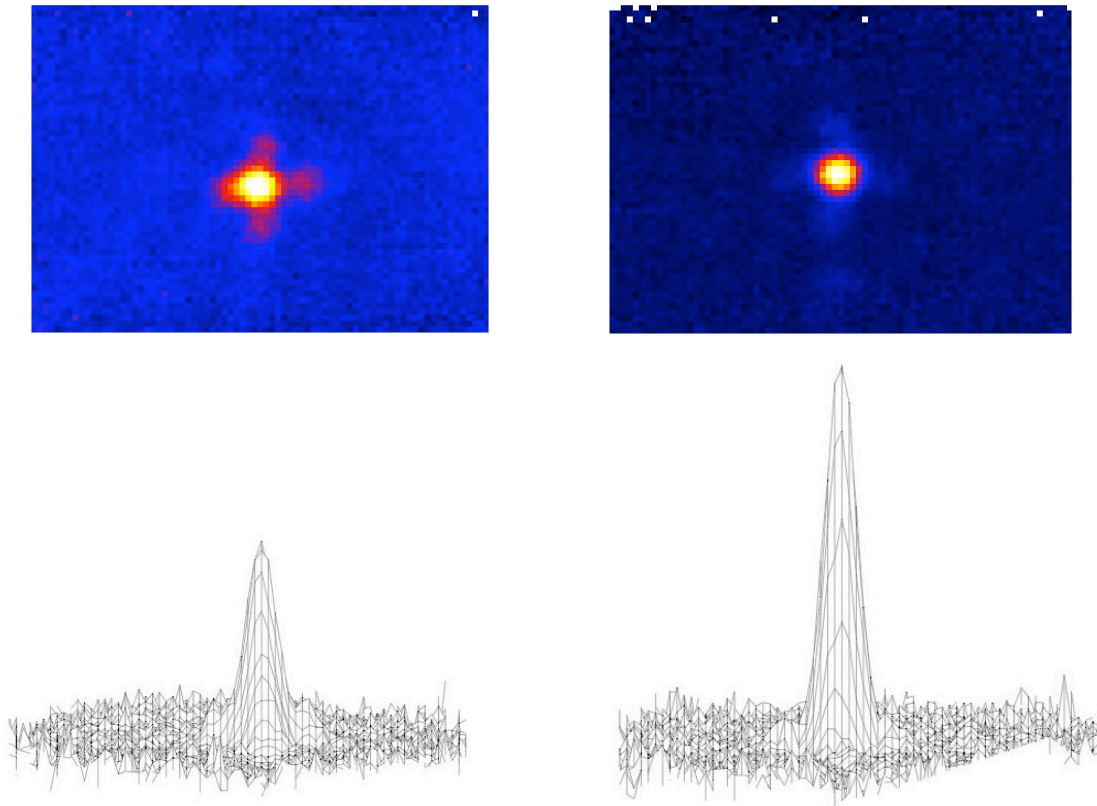


Figure 7. SHARCII Images of Ganymede. Power and 3-D Maps with DSOS Off (left) then DSOS On (right).

Dave Woody's, et al. [2] 1998 RMS surface derivation of the CSO predicted that the best RMS value that can be obtained, considering the primary's small-scale surface errors, is slightly more than 10- μ m at a zenith angle of 20 degrees. The April 2005 holography run was performed with a correction table compiled with the addition of recent holography data. All 99 channels were operating. Figure 8 compares holography maps taken in September 2002, DSOS off, to those taken in April 2005, DSOS on, at similar elevations. The contour level is 10 microns/line. One can clearly see that the deformations were reduced significantly. With the DSOS on, an average of 10- μ m RMS from a zenith angle range of 22 to 63 degrees was achieved. This, in the least, meets the best surface value predicted.

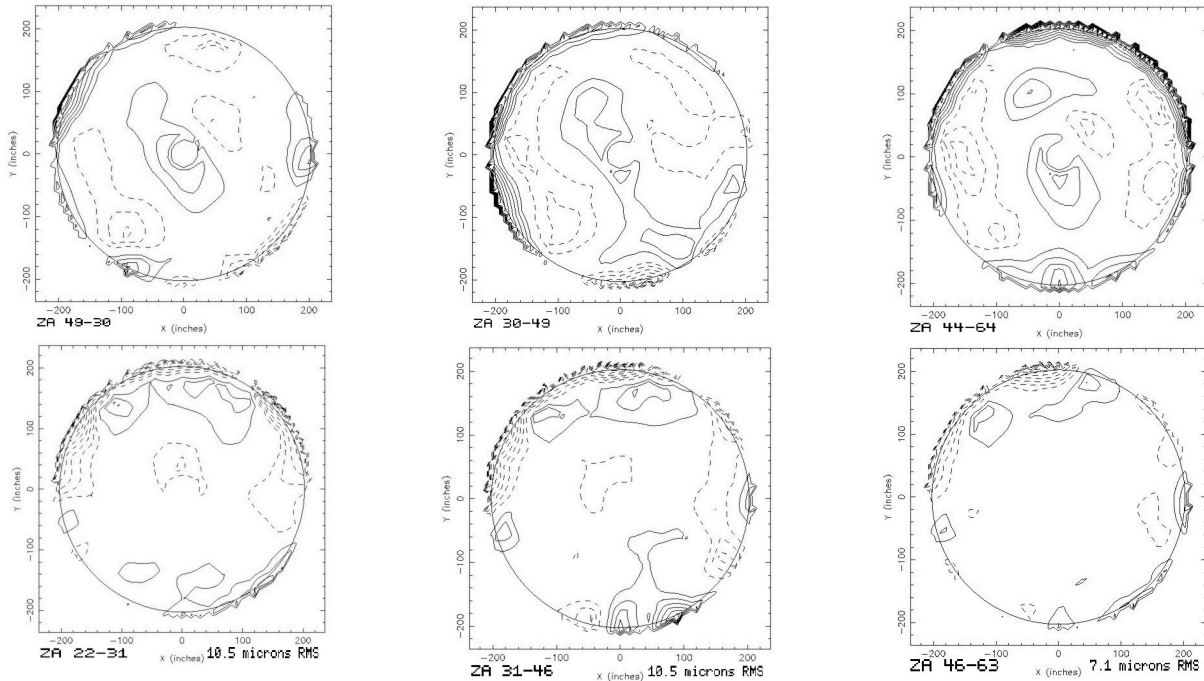


Figure 8. Improvements in Holography Maps – Sept. 2002 (1st Row) vs. Apr. 2005 (2nd Row) at similar elevations.

From these holography results, verification at the 350- μ m-wavelength range was warranted. The 850 GHz Heterodyne Receiver was used to measure the improvements in efficiency. The best percent improvement was as high as 71% with an average of 60% improvement. Figure 9 shows the percent improvements of the two correction tables.



Figure 9. Percent Improvement in Efficiency. Original ZA Lookup Table vs. Updated ZA Lookup Table.

All these measurements were taken with the instruments located on the CSO's cassegrain platform mount. In recent years, there has been an increase in available instruments, resulting to an increase in mounting locations. A second Nasmyth position to the right of the telescope was made available to accommodate for two more instruments. The results meant that SHARCII and the 850 GHz Receiver were to be mounted out on this new platform. With a new optical path, the performance improvement from the DSOS was lessened. Presently the reasons are unknown. A possible explanation is that the optics to the cassegrain platform is well measured and characterized. The second Nasmyth optical path, being newer, needs time to become well measured and characterized. There is still appreciable improvement seen by SHARCII, however, the full benefits on N2 have not been materialized yet.

In February 2006, steps have begun to optimize the DSOS correction tables to accommodate the new optical path. Early results indicate a straightforward revision. This needs to be verified with further engineering runs. Figure 10 shows a visible improvement of Ganymede's received signal, seen by SHARCII with the DSOS on, then with several DSOS channels enhanced.

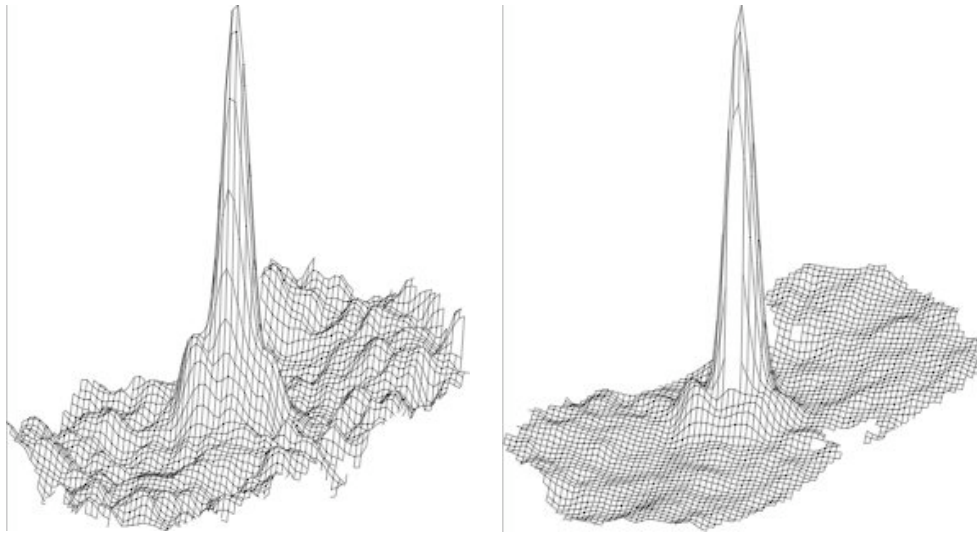


Figure 10. Preliminary N2 Optimization Results – DSOS On (left) then DSOS On w/ Enhanced Channels (right).

6. OBSERVED DISCOVERIES

The DSOS has helped scientists using the CSO to discover an earth-massed planet in Fomalhaut [5], with what looks like its own Kuiper belt. The SHARCII maps are shown in Figure 11. A similar finding was detected in Epsilon Eridani. The DSOS has also helped in the discoveries of new deep field objects, distant galaxies, and also dense cores in their very early evolutionary stage for star formation.

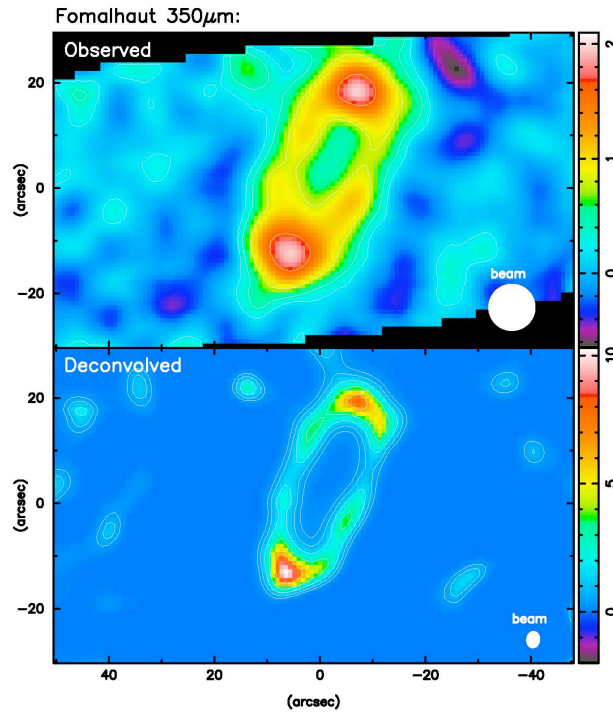


Figure 11. Fomalhaut. – Detection of Earth Massed Planet.

The DSOS helps the CSO obtain higher beam efficiencies and overall sensitivities, enabling multi-wavelength studies of high redshift sources. Alexandre Beelen, et al. [6] was able to resolve dust emissions from high redshift quasars. With SHARCII, Attila Kovacs, et al. [7] studies dust emission properties of deep field galaxies at high z values ($z > 2$). Figure 12 is courtesy of Min Yang at Caltech. These are dusty galaxies at intermediate redshifts ($0.1 < z < 1.0$). Along with Kovacs and Borys, this work is part of a census of all infrared luminous galaxies, at all redshift ranges. It is also an opportunity to learn more about cosmological evolution. Ray Furuya, et al. [8] observed a dense core filament, believed to be a star formation region in Cepheus. Sophia Khan, et al. [9] was one of the early benefactors of the improved sensitivity of SHARCII by the DSOS. They were able to survey IRAS sources and uncover a possibly different process to ultraluminous infrared galaxy (ULIRG) formation. With recent improvements to the DSOS, Colin Borys, et al. [10] detected a unique hyperluminous infrared galaxy at a redshift of $z = 1.325$. The bright far-infrared emissions from this galaxy is not powered by a black hole, as in many cases, but by the extensive star formation activities in the galaxy, about 1000 stars per year! Figure 13 shows a never before seen display of a very long and delicate looking filament in NGC6334, a galactic star formation region. This picture is courtesy of Larry Kirby, U. Chicago, and C. Darren Dowell, JPL/Caltech.

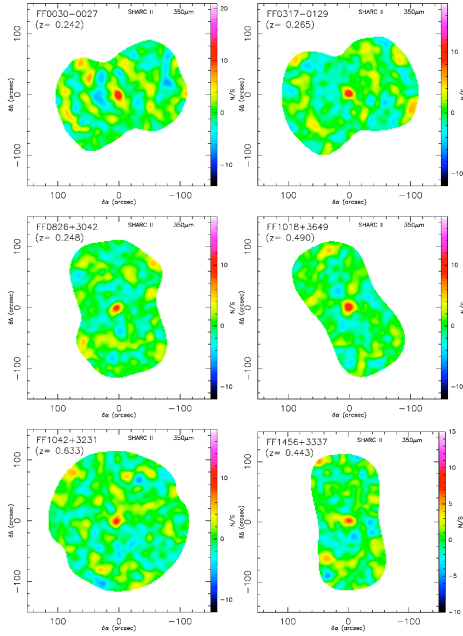


FIG. 1.— Examples of SHARCII detected galaxies in the Stanford sample with $0.1 \leq z \leq 1$

Figure 12. SHARCII images of selected galaxies from the Stanford Sample; PhD thesis work by M. Yang at Caltech.

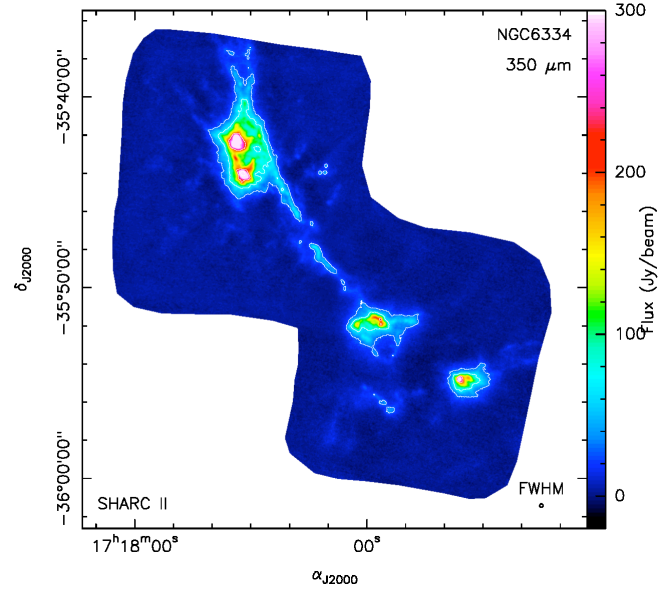


Figure 13. NGC6334 – Galactic Star Formation Region with SHARCII at 350 microns. Courtesy of L. Kirby, U. Chicago, and C.D. Dowell, JPL/Caltech.

7. SUMMARY

The DSOS has proved to be a worthy accomplice for observers at the CSO. It is a unique active optics system for a unique telescope. The DSOS has shown significant improvements in signal power and beam shape in the 350-micron wavelength range. It has been in use for scientific observations since February 2003. With the help of the DSOS, the SHARCII Bolometer Camera and the 850 GHz Heterodyne Receiver are able to detect new weak and/or distant galaxies at the CSO.

ACKNOWLEDGEMENTS

The DSOS was researched, prototyped, designed, and built through a grant from the National Science Foundation, Grant Number: AST 9980846.

REFERENCES

1. R.B. Leighton, “A 10-Meter Telescope for Millimeter and Sub-Millimeter Astronomy,” *Final Technical Report for NSF Grant AST 73-04908*, 1978.
2. D. Woody, E. Serabyn, A. Schinckel, “Measurement, Modeling and Adjustment of the 10.4 m Diameter Leighton Telescopes,” *Proc. SPIE 3357*, pp. 474-485, 1998.
3. E. Serabyn, T.G. Phillips, C.R. Masson, “Surface Figure Measurements of Radio Telescopes with a Shearing Interferometer,” *Applied Optics*, 30(10), pp 1227-1241, 1991.
4. C.D. Dowell, C.A. Allen, S. Babu, M.M. Freund, M. Gardner, J. Groseth, M. Jhabvala, A. Kovacs, D.C. Lis, S.H. Moseley Jr., T.G. Phillips, R. Silverberg, G. Voellmer, H. Yoshida, “Millimeter and Submillimeter Detectors for Astronomy,” *Proc. SPIE 4855*, pp. 73-87, 2003.
5. K.A. Marsh, T. Velusamy, C.D. Dowell, K. Grogan, C.A. Beichman, “Image of Fomalhaut Dust Ring at 350 Microns: The Relative Column Density Map Shows Pericenter-Apocenter Asymmetry,” *The Astrophysical Journal* 620:L47, 2005.

6. A. Beelen, P. Cox, D.J. Benford, C.D. Dowell, A. Kovacs, F. Bertoldi, A. Omont, "350 Micron Dust Emission from High Redshift Quasars," submitted to *The Astrophysical Journal*, 2006.
7. A. Kovacs, S.C. Chapman, C.D. Dowell, A.W. Blain, T.G. Phillips, "SHARC-2 350um Observations of Distant Submillimeter Selected Galaxies," submitted to *The Astrophysical Journal*, 2006.
8. R.S. Furuya, Y. Kitamura, H. Shinnaga, "Detection of dense molecular core in a very early evolutionary stage," submitted to *The Astrophysical Journal*, 2006.
9. S.A. Khan, D.J. Benford, D.L. Clements, S.H. Moseley, R.A. Shafer, T.J. Sumner, "Resolving IRAS 09111-1007 at 350 Microns: A Different Path to ULIRG Formation?" *MNRAS Letters* 359, L10, 2005.
10. C. Borys, A.W. Blain, A. Dey, E. Le Floc'h, B.T. Jannuzil, V. Barnard, C. Bian, M. Brodin, K. Menendez-Delmestre, D. Thompson, K. Brand, M.J.I. Brown, C.D. Dowell, P. Eisenhardt, D. Farrah, D.T. Frayer, J. Higdon, S. Higdon, T. Phillips, B.T. Soifer, D. Stern, D. Weedman, "A Hyperluminous Starburst Galaxy at $Z=1.325$ with Spitzer and SHARC-II," *The Astrophysical Journal* 636, pp.134-139, 2006.